

# PARAMETRIC MODELING OF METAL INERT GAS (MIG) WELDING PROCESS USING SECOND-ORDER REGRESSION MODEL ANALYSIS

E.R. Imam Fauzi<sup>1</sup>, Z. Samad<sup>1</sup>, M.S. Che Jamil<sup>2</sup>, N.M. Nor<sup>1</sup>  
and G.P. Boon<sup>1</sup>

<sup>1</sup>Manufacturing Engineering Group, School of Mechanical Engineering,  
Universiti Sains Malaysia, 14300 Nibong Tebal, Penang, Malaysia.

<sup>2</sup>Dscaff Group, Mont Kiara, 50480 Kuala Lumpur, Malaysia.

Corresponding Author's Email: <sup>1</sup>erif14\_mec009@student.usm.my

**Article History:** Received 11 August 2017; Revised 26 October 2017;  
Accepted 15 December 2017

**ABSTRACT:** Welding parameters play an important role in determining the quality of a weld joint. In this present study, an attempt was made to determine the correlation of the welding parameters and weld quality of MIG welding process using regression analysis of a full factorial design experiment. Welding speed and arc voltage were varied during the fabrication of T-joint AA 6082-T6 aluminium alloys. Weld quality was analyzed in terms of tensile strength and penetration depth. Considering all terms, a linear regression analysis was employed to develop input-output correlation. From the analysis of ANOVA, it is noticeable that welding voltage and the voltage-speed interaction significantly affect both tensile and penetration depth. The developed empirical model to predict tensile strength and penetration depth can yield nearly accurate results, where the percentage error is below 10%, within the range of design environment.

**KEYWORDS:** MIG; Aluminium Alloy; Regression Analysis; Tensile Strength; Penetration Depth

## 1.0 INTRODUCTION

A number of joining techniques, particularly welding processes, have been successfully used to join a variety of structure and components made of aluminium alloys. Since 1940s, fusion welding, especially MIG welding has found extensive use in wide range of industries such as in the construction of aluminium boats, storage tanks, bridge

structures, transport equipment, and general metal works [1]. MIG welding process, also known as Gas Metal Arc Welding (GMAW), is a continuous arc welding process. During the process, an arc is maintained between a continuous solid wire electrode and the work piece, thereby causing a current flow which generates thermal energy in the partially ionized inert gas. The arc and the melt pool are shielded from atmospheric contamination by an inert or active gas. Due to the innate characteristics of this process, MIG welding is commonly used for welding aluminium products in all positions. It is very useful for joints that require deep penetration and narrow heat affected zone (HAZ) [2].

Strength and quality of welded joints depends greatly on the parameter settings used in the welding process. In order to obtain a good welded joint with minimal defects, the process input parameters has to be controlled. Traditionally, the weld input parameters were determined for every new welded product to obtain a good quality weld with required specifications. This demands a time-consuming trial and error effort, thus increasing production cost. Recently, application of various optimization methods such as design of experiment, evolutionary algorithms and computational network, in order to define the desired output variables are widely used and adapted for many applications in different areas. Factorial design technique is one of frequently adapted application for modeling and optimizing a process [3]. To date, considerable efforts have been made in the application of factorial design technique in welding process that aimed to increase weld quality. Koganti et al. [4] have employed a full factorial design to determine optimized parameters in MIG welding of AA 5754 aluminium alloys. The effects of process parameters such as power input, pulse frequency and gas flow rate on tensile shear strength have been investigated. It is found that the power input and gas flow rate directly influence the lap shear load to failure. Pine et al. [5] studied variety of factors, namely; sheet thickness, strength of steel, section design, weld end and section area of spot welded, adhesively bonded and weld-bonded box sections using factorial design technique. An experimental and numerical study was presented to determine the torsional stiffness, ultimate strength and elastic limit of each joining type. It was concluded that the most important factor influencing the elastic limit and ultimate strength

was the steel strength. In addition, the torsional stiffness can be enhanced by adjusting the joining technique from 50 mm pitch spot welds to the adhesive joint or by increasing the section area. Kim et al. [6] have presented factorial design to develop a correlation of robotic GMAW process parameters (welding voltage, welding speed and arc current) to three output responses (bead width, bead height and penetration) in bead-on-plate welding of AS 1204. From the analysis, it was reported that all process parameters influenced the responses and the developed models were able to predict the responses with 0-25% accuracy.

Another attempt was made by Murugan and Parmar [7]. They adapted a mixed levels factorial design technique to develop a mathematical model for predicting the weld-bead geometry in the deposition of 316L stainless steel onto IS2062 steel. The developed models could be implemented into automatic robotic surfacing in a form of program in order to obtain the desired output. Additionally, the effects of each factor on the weld features were successfully determined. Ganjigatti et al. [8] developed a mathematical model of MIG welding process using statistical approach. Both linear and non-linear regression analyses on the MIG welding of mild steel plate were carried out using full factorial design of experiments. It was found that all three approaches of linear regression analysis have slightly outperformed the non-linear regression in terms of average Response Mean Standard deviation of prediction. Murugan and Gunaraj [9] developed mathematical models using a five-level factorial technique to analyze various process control parameters in submerged arc welding of structural steel pipes. The aim was to relate the important process control variables, namely welding voltage, wire feed rate, welding speed and nozzle-to-plate distance, to a few important bead quality parameters such as penetration, reinforcement, bead width and total volume of bead.

In recent study by Patil and Waghmare [10], the influence of welding parameters such as welding current, voltage and speed on ultimate strength of AISI 1030 mild steel during welding were investigated based on Taguchi method. It is found that welding current and welding speed were statistically significant and have a major influence on tensile strength. Another study was made by Haragopal

et al. [11] to investigate the optimized conditions of weldment AA 65032 aluminium alloys, used for construction of aerospace wings. Experimental analysis was conducted using Taguchi method by considering the gas pressure, current, groove angle and pre-heat temperature as process parameters. In this case, optimum condition to enhance the mechanical properties was found by signal-to-noise analysis and mean response calculation. Meanwhile, Sreeraj et al. [12] presented a second-order regression model of stainless steel cladding deposited by MIG process, to predict four critical dimensions of bead geometry. A central composite rotatable design with full replication was implemented as experimental concept and 'fmincon' function was used to optimize the process parameters.

The present study highlights the effect of softening behaviour on welded specimens, which is often referred to the consequent of metallurgical transformation during welding. In most aluminium alloy weldments, the fusion region is the weakest zone. A notable exception is observed in 6000 series aluminium alloy, where the weakest zone is experienced in HAZ. For 6000 series aluminium alloys, the softening effect can lead to the reduction of proof strength in the heat affected zone (HAZ) on the order of 30 % - 50 %. Additionally, the HAZ normally extends between 10mm-30mm from the centre of the weld [13]. Therefore, it is essential to study the sensitivity of welding parameters on softening behaviour of welded aluminium alloy joint. In this study, full factorial design with three levels was implemented to identify the critical factors of MIG welding parameters. A multiple linear regression analysis was used to fit a polynomial experimental data. The aim of this study is to correlate the MIG welding parameters (welding voltage and welding speed) to the mechanical properties of the joints. A regression model based on the experimental data was developed to predict the performance responses of the MIG process. The accuracy of the model was validated experimentally and some important observations were made.

## 2.0 METHODOLOGY

### 2.1 Experiment Setup

The material used was AA 6082-T6 aluminium alloy with thickness of 5 mm. AA 6082 is relatively new material which can provide high strength properties, satisfactory corrosion resistance, good weldability and machining performance [14]. Depending on material form and heat treatment, 6082 alloy can possess until 12 % - 19 % higher strength for characteristic values of ultimate tensile strength compared to another 6000 series alloy [15]. The chemical composition of the materials was analyzed using Energy-dispersive X-ray Spectroscopy (EDX) and presented in Table 1. Specimens were cut using water jet to prevent any thermal force exerted on the specimen that can alter the microstructure.

Table 1: Chemical composition of aluminium alloy AA 6082

Chemical	Mn	Fe	Mg	Si	Cu	Zn	Ti	Cr	Al
% Present	0.4 - 1.0	±0.5	0.6 -1.2	0.7-1.3	±0.1	±0.2	±0.1	±0.25	Balance

Single-sided semi-automated welding of T-joint was conducted by using Kemppomat 2500 welding machine and KUKA KR6 robotic arm as shown in Figure 1. A single pass welding was performed with the presence of pure Argon (99 %) as shielding gas to protect the molten pool from atmospheric contamination. A groove of 45° was designed to ensure full penetration of the weld seam. A filler wire of type AA 4043 (~ 5 % Si) was used in this welding process due to the ability of reducing crack sensitivity. The MIG process parameters are; Argon flow rate = 20 litre/min, torch angle = 20°, wire feeding rate = 6.5 m/min, voltage variation = 25.5 V, 28.3 V, 31.4 V and welding speed variation= 0.4 m/min, 0.45 m/min, 0.5 m/min.

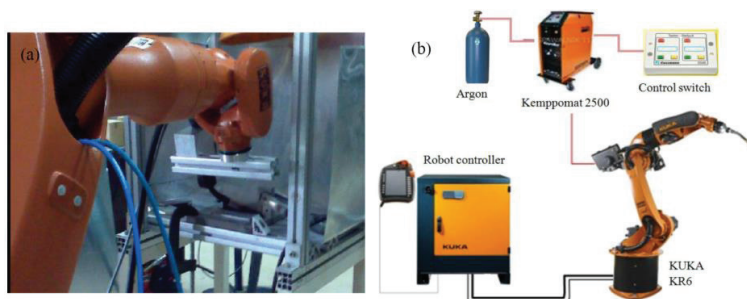


Figure 1: (a) Experiment setup and (b) Schematic diagram of experimental setup

## 2.2 Measurement of Responses

Sub-sizes dogbone tensile specimens were prepared from the weld region in a longitudinal direction according to the ASTM E8 standard [16] to analyze the tensile properties of welded material (as shown in Figure 2). Tensile test was performed using Shimadzu Universal Tensile Machine with a constant speed of 0.48 mm/min. In accordance to the American Welding Society (AWS) standard [17], depth of penetration was measure as root penetration as shown in Figure 3. The measurement of penetration was carried out using Scanning Electron Microscope (SEM) under 25X magnificent.

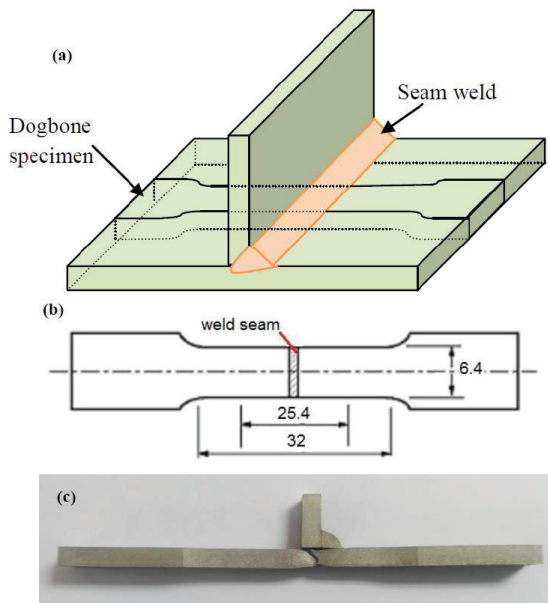


Figure 2: (a) Cross joint of tensile specimens, (b) Basic dimensions of tensile test sub-specimen according to ASTM-E8 and (c) Tensile test specimen of T-joint showing the fractured region

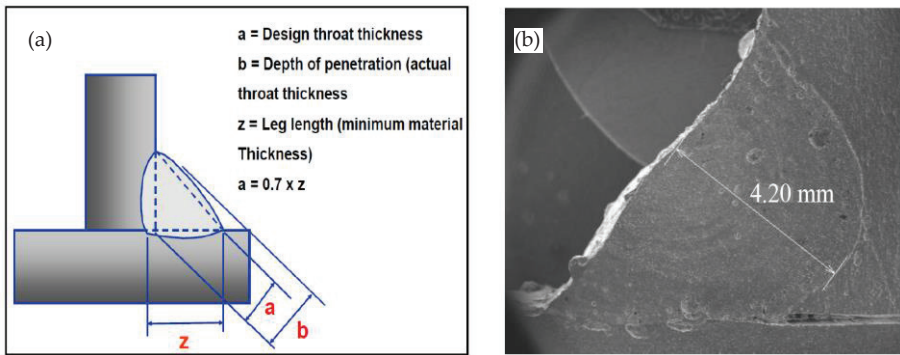


Figure 3: (a) Penetration depth measurement according to AWS standard and (b) Measurement of penetration under SEM (25X magnificant)

### 2.3 Full Factorial Design Experiment

There are two input parameters and each of them has been set at three level variations. Thus, a total of 9 combinations with 2 replications were taken into account according to the full factorial design experiments (DOE). Trial runs were conducted by varying one of the process parameters at a time, while keeping the rest of them at constant value. The working range was decided by inspecting the weld seam for a smooth appearance and the absence of any visible defects. Table 2 presents the experimental data collected based upon the proposed DOE.

Table 2: Experimental data collected as per proposed DOE

Sample no	Voltage (V)	Speed (m/min)	Replication 1		Replication 2		Average	
			Stress (MPa)	Penetration depth (mm)	Stress (MPa)	Penetration depth (mm)	Stress (MPa)	Penetration depth (mm)
1	23.0	0.40	208.069	3.26	207.877	3.41	207.973	3.34
2	23.0	0.45	210.216	3.54	208.442	3.23	209.329	3.39
3	23.0	0.50	214.700	3.05	213.671	3.10	214.186	3.08
4	25.5	0.40	206.778	4.01	198.716	3.68	202.747	3.85
5	25.5	0.45	199.327	3.92	193.869	4.20	196.598	4.06
6	25.5	0.50	209.331	3.92	202.608	4.11	205.970	4.02
7	28.3	0.40	204.841	3.57	210.408	3.68	207.625	3.63
8	28.3	0.45	211.720	3.28	208.394	3.31	210.057	3.30
9	28.3	0.50	215.775	2.97	211.397	2.83	213.586	2.90

## **2.4 Regression analysis**

In this work, a multiple linear regression model with two predictor variables was developed to characterize the correlation between the inputs and outputs. The method of least square estimation was used to estimate the regression coefficients in a multiple linear regression model. The low, intermediate and high levels were denoted by -1, 0 and 1, respectively in order to facilitate a fitted regression model. From the collection of data in Table 2, a general second-order model can be expressed as:

$$y = \beta_0 + \beta_1 x_1 + \beta_2 x_2 + \beta_{12} x_1 x_2 + \beta_{11} x_1^2 + \beta_{22} x_2^2 + \epsilon \quad (1)$$

Where  $y$  represents the response,  $x_1$  represents the welding voltage,  $x_2$  represents the welding speed, parameters  $\beta_j$  represents the regression coefficient of each term and  $\epsilon$  represents the error.

## **3.0 RESULTS AND DISCUSSION**

Commercial statistical software MINITAB was used for analysis of the measured responses and determining the best fits model. The sequential f-test and the analysis of variance (ANOVA) were used to test the adequacy of the model.

### **3.1 Analysis of Tensile Strength**

The analysis of variance (ANOVA) for the tensile strength is summarized in Table 3. It is suggested that the quadratic relationship where the additional terms are significant was fit for the analysis. It is noticeable that welding voltage significantly affects the tensile strength. Clearly, the adequacy measures of  $R^2$  and adjusted  $R^2$  are likely large, which is indicated that the most of the variability in tensile strength can be explained by the predictors. The associated small p-values reflect that the model terms are statistically significant. The voltage-speed interaction F-ratio has a p-value of 0.010, indicating some interaction between both factors.



Table 3: The ANOVA results for the tensile strength model

Source of variation	SS <sup>a</sup>	DF <sup>b</sup>	MS <sup>c</sup>	F-ratio	P-value
Regression	425.91	5.00	85.18	6.91	0.003
A, Voltage	0.19	1.00	0.19	0.02	<0.00
B, Welding speed	79.02	1.00	79.02	6.41	0.11
AB	0.01	1.00	0.01	<0.00	0.078
A <sup>2</sup>	301.72	1.00	301.72	24.45	<0.00
B <sup>2</sup>	44.97	1.00	44.97	3.65	0.08
Error	148.03	12.00	12.34		
Total	573.94	17.00			
R <sup>2</sup> = 74.2%			R <sup>2</sup> (adj) = 63.5%		
<sup>a</sup> Sum of square	<sup>b</sup> Degree of freedom		<sup>c</sup> Mean square		

The graph of the average response at each treatment combination is shown in Figure 4. The significant interaction is indicated by the lack of parallelism of the lines. Generally, higher tensile stress is attained at higher speed regardless of voltage level. Changing from low speed to higher speed, the tensile strength may increase in the case of lower and higher voltage. This effect could be attributed to the following reason. Increasing the welding speed leads to the lower contact time of energy deposition, causing low heat input to the weld zone. Due to high thermal conductivity of aluminium alloy, the heat dissipates quickly from the weld region to the surrounding material. The rapid cooling rate of welded material, in turn produces grains with narrower arm spacing in the welded region. Meanwhile in the HAZ, which adjacent to the fusion boundary, complete dissolution of Mg<sub>2</sub>Si hardening precipitates occur due to higher temperature attained. The strength loss effect in this region is less severe, because the microstructure will tend to age in natural manner. On the other hand, the HAZ near to the base metal is exposed to a range of temperatures where the aging and overaging phenomena may occur. As a result, either partial dissolution of precipitates or precipitate coarsening will dominate this region due to microstructural transformation. The extent of the dissolution or coarsening will vary as a function of peak temperature. Therefore, as a consequence of lowering the heat input, cooling rate will increase, thus a narrower overaging zone is obtained [18-19]. This microstructure characteristic promotes higher value in tensile strength. For the case of intermediate voltage, the stability of tensile strength is unpredictable. Considering above data, the regression model for tensile strength, which can be used for prediction within the same design space are expressed as follows:

$$\text{Tensile strength} = 1262 - 63.58A - 1148.80B + 1.24A^2 + 1341.20B^2 - 0.27AB \quad (2)$$

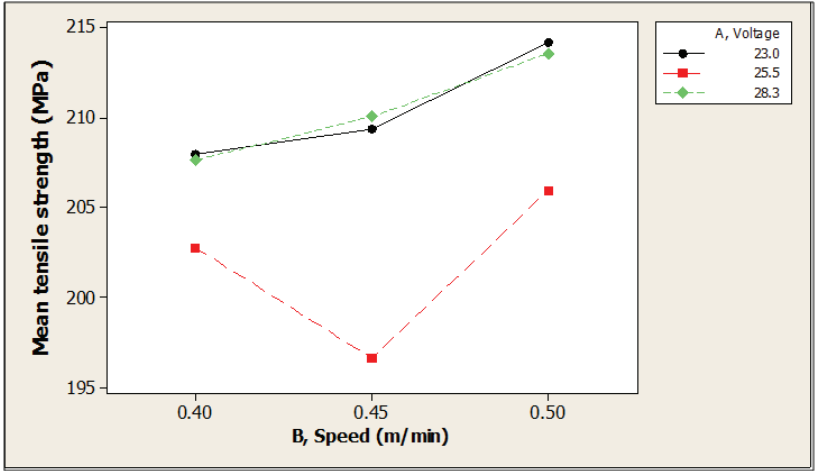


Figure 4: Voltage-welding speed interaction plot for tensile strength

### 3.2 Analysis of Penetration Depth

The second-order model for the penetration depth analysis can be written as:

$$\text{Penetration depth} = -80.9 + 5.58A + 62.00B - 0.10A^2 - 45.70B^2 - 0.92AB \quad (3)$$

Summary of the ANOVA of the quadratic model is presented in Table 4. It can be seen that the adequacy measures of  $R^2$  and adjusted  $R^2$  are reasonably high, which is about 83.1 % and 76.1 %, respectively. The associated p-value of the regression model, which is less than 0.05 indicates that the model can be considered as statistically significant. The main effect of welding voltage along with the interaction effect of voltage-speed is considered significant. Nevertheless, the main effect of welding speed is added to the model terms to support hierarchy.

Table 4: The ANOVA results for the penetration depth analysis

Source of variation	SS <sup>a</sup>	DF <sup>b</sup>	MS <sup>c</sup>	F-ratio	P-value
Regression	2.38	5.00	0.48	11.78	<0.00
A, Voltage	0.00	1.00	0.00		<0.00
B, Welding speed	0.22	1.00	0.22	5.50	0.13
AB	0.12	1.00	0.12	3.00	0.01
A <sup>2</sup>	0.98	1.00	0.98	24.50	<0.00
B <sup>2</sup>	0.05	1.00	0.05	1.25	0.02
Error	0.48	12.00	0.04		
Total	2.86	17.00			
R <sup>2</sup> = 83.1%			R <sup>2</sup> (adj) =76.0%		
<sup>a</sup> Sum of square			<sup>b</sup> Degree of freedom		<sup>c</sup> Mean square

Figure 5 illustrates the interaction plot between welding voltage and welding speed for penetration depth analysis. Generally, better penetration depth is achieved at low welding speed except for the case of intermediate voltage supply. This is due to the fact that with increase in welding speed, the contact time of energy deposition is reduced. Hence, less heat was experienced during the welding. Consequently, less amount of material being melted and thus resulting to narrower penetration [20]. It is apparent that penetration in between 3.2 mm to 4.0 mm can be attained at lower welding speed regardless of voltage levels. In the case of higher voltage, the penetration depth is decreased significantly as the speed increases. A slight increase in penetration depth can be observed for the case of lower voltage and intermediate speed.

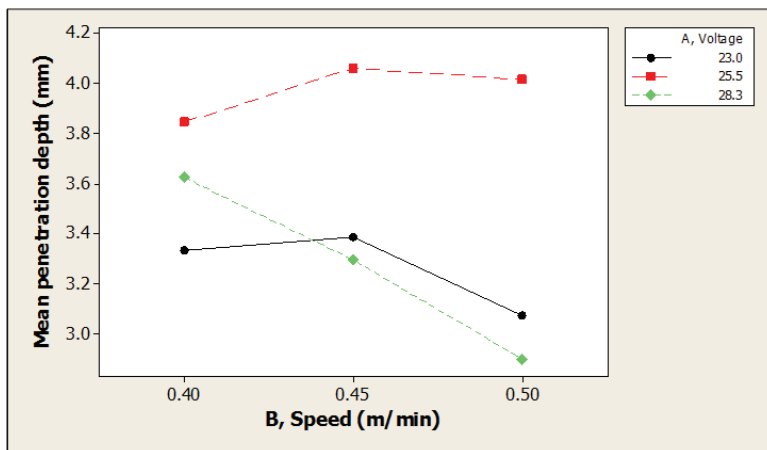


Figure 5: Voltage-welding speed interaction plot for penetration depth

### 3.3 Validation of Empirical Model

In order to validate the developed empirical models, three confirmation experiments were conducted. The welding conditions were chosen randomly to avoid any violation in variability. For each case, experiments were repeated twice, and the average responses were calculated. Table 5 presents the experimental results, predicted values and calculated percentage errors of validation experiments. The results show that the errors between predicted and experimental data in experiment 1 and 2 are relatively small (below 10 %), which suggest that the developed empirical models can yield nearly accurate results within the ranges for which the equations are derived. However, in experiment 3, where welding conditions were chosen outside the design space, the percentage error between estimated and actual data is comparatively higher. These figures indicate that the empirical models are not adequate to predict data range outside the design environment.

Table 5: Experiment data, predicted values and percentage errors of validation experiment

Case	Voltage (V)	Speed (m/min)		Tensile stress (MPa)	Penetration depth (mm)
1	23	0.35	<i>Exp.</i>	197.36	3.31
			<i>Pred.</i>	215.66	3.24
			<i>Error (%)</i>	9.30	2.10
2	25.5	0.35	<i>Exp.</i>	212.6	4.65
			<i>Pred.</i>	206.83	4.25
			<i>Error (%)</i>	2.70	8.60
3	31.4	0.4	<i>Exp.</i>	210.09	1.58
			<i>Pred.</i>	245.73	1.20
			<i>Error (%)</i>	16.90	24.10

### 4.0 CONCLUSION

This study was aimed to investigate the relationship between weld quality in terms of tensile strength and deep of penetration, and welding parameters, namely welding voltage and welding speed. Three levels factorial technique was employed to design the experimental procedure and a multiple regression method was used for analysis. Second-order empirical models to predict the responses were developed and validated experimentally. From the analysis of

ANOVA, it is noticeable that welding voltage and the voltage-speed interaction significantly affect both tensile and penetration depth. It is reported that the developed empirical model to predict tensile strength and penetration depth can yield nearly accurate results, where the percentage error is below 10 %, within the range of design environment. It is found that higher tensile stress was attained at higher speed and penetration in between 3.2 mm to 4.0 mm can be obtained at lower welding speed regardless of voltage levels. The published data for this study remains small and further expansion of the design basis is clearly needed to improve the developed empirical model.

## ACKNOWLEDGMENTS

The authors acknowledge the support from University Science Malaysia (USM) through research grant 1001/PMEKANIK/814235. The financial support under MyBrain15 from Malaysia Ministry of Education (MoE) is greatly appreciated. They also wish to thank Mr. Mohd Ashamuddin Hashim for providing technical support to conduct the analysis.

## REFERENCES

- [1] G. Mathers, *The Welding of Aluminium and its Alloys*. England: Woodhead Publishing Limited, 2002.
- [2] A. Lakshminarayanan, V. Balasubramanian, and K. Elangovan, "Effect of welding processes on tensile properties of AA6061 aluminium alloy joints," *International Journal of Advanced Manufacturing Technology*, vol. 40, pp. 286–296, 2009.
- [3] K.Y. Benyounis and A.G. Olabi, "Optimization of different welding processes using statistical and numerical approaches - A reference guide," *Advances in Engineering Software*, vol. 39, pp. 483–496, 2008.
- [4] R. Koganti, C. Karas, A. Joaquin, D. Henderson, M. Zaluzec and A. Caliskan, "Metal Inert Gas (MIG) welding process optimization for joining aluminium sheet material using OTC/DAIHEN equipment," in *ASME 2003 International Mechanical Engineering Congress and Exposition*, Washington DC, USA, 2003, pp. 409–425.

- [5] T. Pine, M. Lee, and T. Jones, "Factors affecting torsional properties of box sections.," *Ironmarking & Steelmarking*, vol. 25, pp. 205–209, 1998.
- [6] I. Kim, K. Son, Y. Yang, and P. Yaragada, "Sensitivity analysis for process parameters in GMA welding processes using a factorial design method," *International Journal of Machine Tools and Manufacture*, vol. 43, pp. 763–769, 2003.
- [7] N. Murugan and R. Parmar, "Effects of MIG process parameters on the geometry of the bead in the automatic surfacing of stainless steel," *Journal of Materials Processing Technology*, vol. 41, pp. 381–398, 1994.
- [8] J.P. Ganjigatti, D.K. Pratihari, and A. Roychoudhury, "Modeling of the MIG welding process using statistical approaches," *International Journal of Advanced Manufacturing Technology*, vol. 35, pp. 1166–1190, 2008.
- [9] N. Murugan and V. Gunaraj, "Prediction and optimization of weld bead volume for the submerged arc process — Part 2," *Welding Research Supplement*, pp. 331–338, 2000.
- [10] S. Patil and C. Waghmare, "Optimization of MIG welding parameters for improving strength of welded joints," *International Journal of Advanced Engineering Research and Studies*, vol. 2, pp. 14–16, 2013.
- [11] G. Haragopal, P.V.R. Ravindra Reddy, G. Chandra Mohan Reddy, and J.V. Subrahmanyam, "Parameter design for MIG welding of Al-65032 alloy using Taguchi technique," *Journal of Scientific & Industrial Research*, vol. 70, pp. 844–850, 2011.
- [12] P. Sreeraj, T. Kannan, and S. Maji, "Prediction and optimization of weld bead geometry in gas metal arc welding process using RSM and fmincon," *Journal of Mechanical Engineering Research*, vol. 5, pp. 154–165, 2013.
- [13] M. Collette, "The impact of fusion welds on the ultimate strength of aluminum structures," in *10th International Symposium on Practical Design of Ships and Other Floating Structures (PRADS)*, Houston, Texas, USA, 2007.
- [14] F. Mazzolani, *Aluminium Alloy Structures, 2<sup>nd</sup> Edition*. London: Chapman & Hall, 1995.
- [15] CEN European Community for Standardization, "Eurocode 9 Design of aluminium structures. Part1-1: General structural rules. EN-1999-1-1," Brussels, 2007.

- [16] ASTM International, "E8/E8M standard test methods for tension testing of metallic materials," West Conshohocken, US, 2010.
- [17] American Welding Society, "ANSI/AWS A3.0-94 Standard welding terms and definitions," Florida, US, 1999.
- [18] T. Ma and G. den Ouden, "Softening behaviour of Al-Zn-Mg alloys due to welding," *Materials Science and Engineering: A*, vol. 266, pp. 198–204, 1999.
- [19] K. Easterling, *Introduction to the Physical Metallurgy of Welding*, 2<sup>nd</sup> Edition. Netherlands: Elsevier, 2013.
- [20] B. Das, B. Debbarma, R.N. Rai, and S.C. Saha, "Influence of Process parameters on depth of penetration of welded joint in MIG welding process," *International Journal of Research in Engineering & Technology*, vol. 2, pp. 220–224, 2013.

